PERGAMON

Journal of Structural Geology 24 (2002) 1603–1618

JOURNAL OF STRUCTURAL GEOLOGY

www.elsevier.com/locate/jstrugeo

Structural evolution of an antiformal window: the Scheiblingkirchen Window (Eastern Alps, Austria)

Ernst Willingshofer[a,*], Franz Neubauer[b]

[a]*Faculty of Earth and Life Sciences, Vrije Universiteit, De Boelelaan 1085, 1081 HV Amsterdam, The Netherlands*
[b]*Institut für Geologie und Paläontologie, Universität Salzburg, Hellbrunnerstrasse 34, 5020 Salzburg, Austria*

Received 8 May 2001; revised 2 November 2001; accepted 15 November 2001

Abstract

The Scheiblingkirchen window, a Lower Austroalpine tectonic window at the eastern margin of the Eastern Alps (Austria) was formed during Late Cretaceous continent–continent collision. Structural investigations including structural mapping, microstructural studies and texture analysis revealed a decompression-related three-stage tectonic history of Lower Austroalpine units during the formation of the Scheiblingkirchen window.

(1) Intra-Lower Austroalpine nappe stacking was by top-to-the-N out-of-sequence thrusting of the Kirchberg fold nappe over the Wechsel nappe under lower greenschist facies metamorphic conditions. The structural expression of the stacking event (D_1) comprises a penetrative foliation containing a N–S trending stretching lineation, isoclinal recumbent folds trending subparallel to the stretching lineation and ultramylonites. Quartz and calcite microstructures indicate that dynamic recrystallization processes accompanied deformation. Their commonly moderately developed lattice preferred orientation record dominant slip on the prism and rhomb planes parallel to $\langle a \rangle$.

(2) Subsequent exhumation of previously stacked rocks is related to the formation of foliation-parallel mylonitic shear zones within an E–W extensional regime (D_2). Microstructures and textures suggest similar deformation temperatures during thrusting and extension.

(3) A superimposed phase of NW–SE oriented horizontal shortening (D_3) was accommodated by large- and small-scale upright folding of the area around NE–SW trending axes and by backthrusting leading to the antiformal doming of the Scheiblingkirchen Window. Subsequent subvertical flattening resulting from the shortening phase led to the formation of NE–SW trending, outcrop-scale open recumbent folds. Low temperature deformation conditions as inferred from the low degree of recrystallization of quartz and calcite aggregates and the dominance of glide on the basal planes point to a cooling-related deformation event.

Keywords: Eastern Alps; Fold nappe; Kinematics; Lattice preferred orientation; Microstructures

1. Introduction

Close to the transition to the Neogene Pannonian Basin, the Eastern Alps of Austria expose a succession of rock units that have been assembled during Cretaceous and Tertiary orogenic phases. From footwall to hanging wall these include: the Penninic unit of oceanic origin and the Lower-, Middle-, and Upper Austroalpine units, all of continental origin (Fig. 1). Their present-day configuration is explained by Cretaceous stacking of Austroalpine units and subsequent subduction of the Penninic Ocean (e.g. Frisch, 1979; Dallmeyer et al., 1998; Willingshofer et al., 1999a; Neubauer et al., 2000 and references therein). Thrust imbrication occurred by footwall propagation of the thrust planes along a basal master detachment during the Cretaceous, as indicated by the structurally downward younging of geochronological ages from mylonitic rocks (e.g. Dallmeyer et al., 1996, 1998; Liu et al., 2001). Independent evidence for the Cretaceous (Eoalpine) age of these nappe tectonics is given by the intercalation of Permian and Mesozoic cover sequences between thrust sheets (e.g. Tollmann, 1977) and the deposition of Turonian to Eocene syn-orogenic sedimentary sequences sealing thrust planes (Wagreich, 1993; Neubauer et al., 1995; Faupl and Wagreich, 1996, 2000).

Top-to-the-W to NW kinematics have been inferred for the stacking of Austroalpine units (e.g. Ratschbacher et al., 1989; Neubauer et al., 1992; Froitzheim et al., 1997; Müller et al., 1999). Subsequent top-to-the-N shearing has been reported from ductile shear zones (Plattengneiss) of the Middle Austroalpine unit (Krohe, 1987), from intra-Lower Austroalpine basement and cover series at the eastern margin of the Eastern Alps (Neubauer et al., 1992) and from the western Austroalpine plate margin (Ring et al., 1988). Similar top-to-the-N thrust kinematics, pre-dating

* Corresponding author. Tel.: +31-20-44-47353; fax: +31-20-646-2457.
E-mail address: wile@geo.vu.nl (E. Willingshofer).

0191-8141/02/$ - see front matter
PII: S0191-8141(01)00161-4

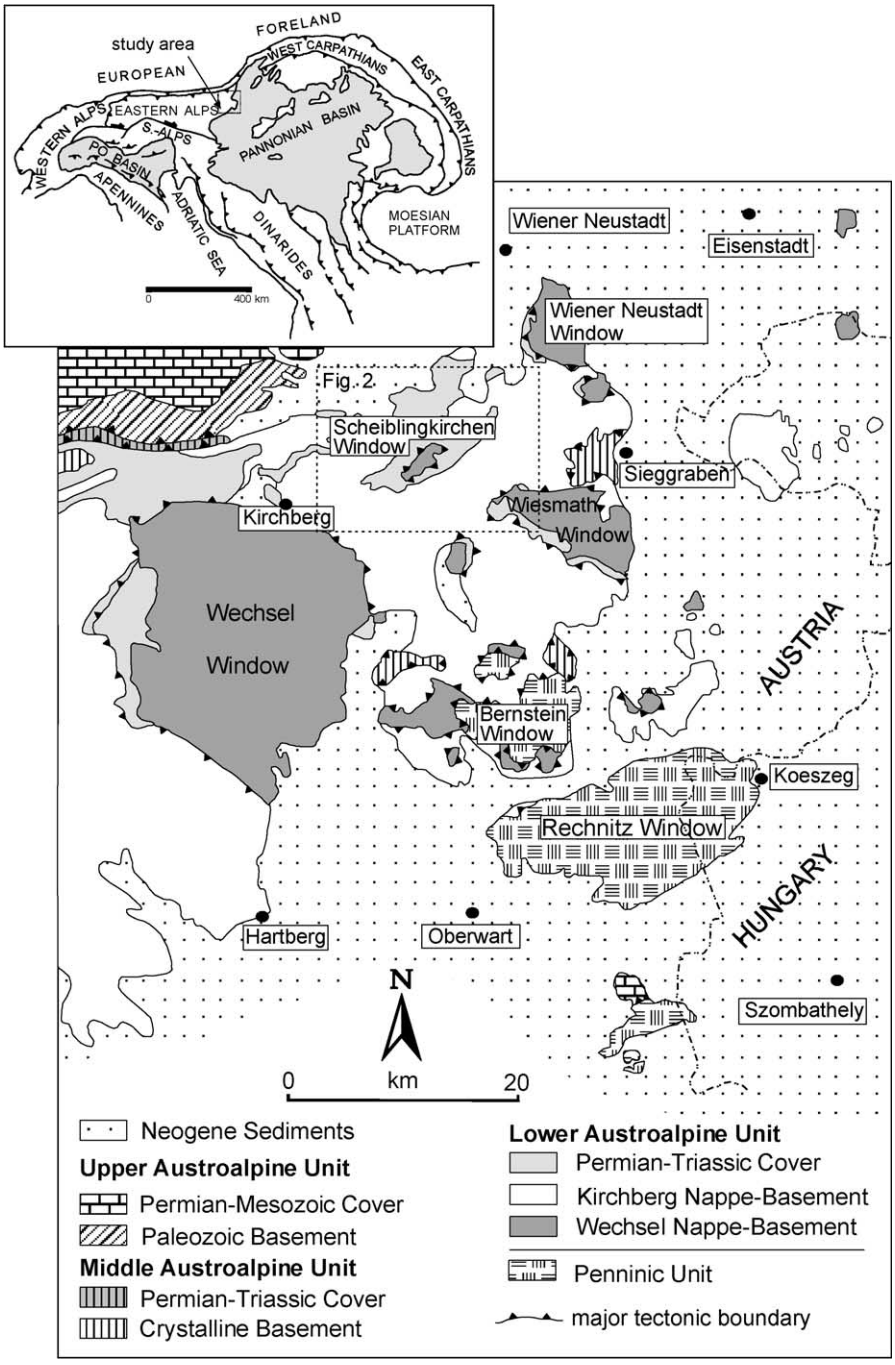

Fig. 1. Simplified tectonic map of the eastern margin of the Eastern Alps (modified after Tollmann, 1978).

Oligocene and younger deformation events, have been described by Ratschbacher et al. (1990) from the underlying Penninic units exposed in for example the Rechnitz Window (Fig. 1).

The top-to-the-N shearing event is poorly documented and not well understood in the context of Late Cretaceous collisional tectonics in the Eastern Alps, and thus, is frequently ignored in tectonic reconstructions. In this study, we present new map- to micro-scale data and results of texture analysis performed on quartz and calcite together constraining the structural and kinematic evolution of Lower Austroalpine units close to the Pannonian Basin. An important reorientation of the regional stress field must have occurred during the Late Cretaceous to account for top-to-the-N directed internal deformation of the Lower Austroalpine units. Subsequent tectonic window formation through folding and thrusting took place under decreasing temperature and pressure conditions.

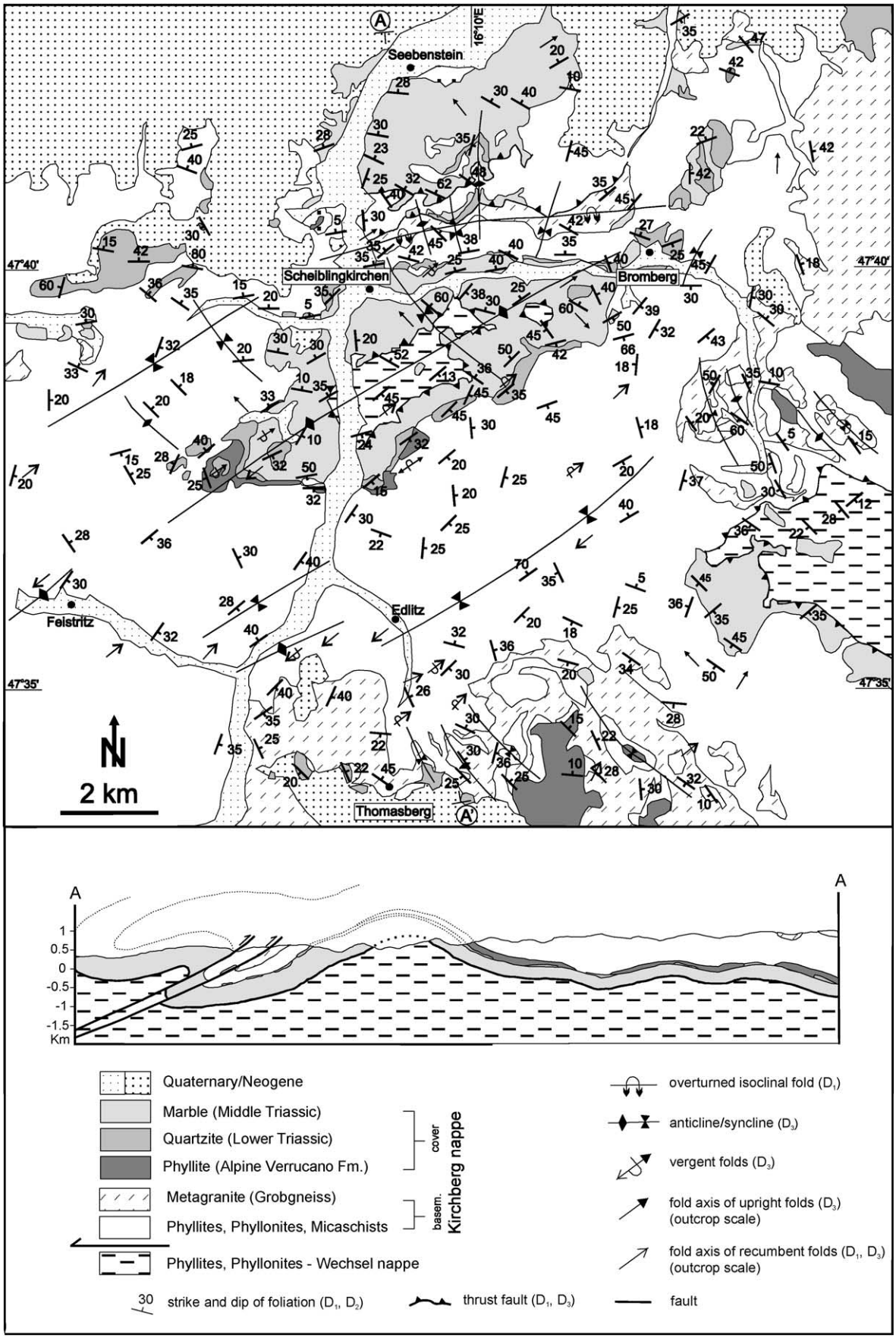

Fig. 2. Structural map of the study area.

2. Geologic setting

Eight tectonic windows within the Lower Austroalpine nappe complex at the eastern margin of the Eastern Alps characterize the geology adjacent to the eastward deepening Pannonian Basin (Fig. 1). All windows expose rocks of the Wechsel nappe beneath the Kirchberg nappe (Tollmann, 1978).

In the case of the Scheiblingkirchen window, phyllites to phyllonitc micaschists of the Wechsel nappe, exposed in its centre (Tollmann, 1977, 1978; Fuchs, 1990), are surrounded and overlain by rocks of the Kirchberg nappe consisting of: (1) a series of monotonous quartz-rich micaschists, quartz–phyllites and locally lenses of amphibolite, (2) a coarse-grained metagranite, containing up to 8 cm K-feldspar phenocrysts, known as 'Grobgneiss', which displays a complex spatial relationship with the micaschist series, and (3) Permian to Scythian clastics and Triassic carbonates, which represent the sedimentary cover of the Kirchberg nappe (Fig. 2). This nappe displays the geometry of a flat-lying fold nappe with an approximately E-trending fold axis pointing northward overturning during fold nappe formation (Fig. 2). The nature of the Kirchberg nappe is illustrated by the inverse layering of the sedimentary cover series in the area of Scheiblingkirchen, which are in particular: (1) Anisian marbles, dolomites and rauhwackes, (2) Permian–Scythian quartzites (Semmering Quartzite), and (3) a series of Scythian metaclastics and metavolcanics (Alpine Verrucano Formation: Riedmüller, 1967; Wieseneder, 1971; Tollmann, 1978; Fuchs, 1990).

Pre-Alpine metamorphism within the basement of the Wechsel and Kirchberg nappes reached greenschist and amphibolite facies conditions during the Variscan orogeny, respectively (Wieseneder, 1971; Neubauer and Frisch, 1993; Frey et al., 1999; Müller et al., 1999). Alpine lower greenschist facies metamorphism is documented within these lithologies as an intense retrogression, whereas the Permo–Triassic rocks display prograde metamorphism (e.g. Fuchs, 1962; Riedmüller, 1967). Radiometric and petrologic data point to a higher degree of the Alpine metamorphic overprint within the hanging wall Kirchberg nappe (Dallmeyer et al., 1996; Müller et al., 1999). Rb/Sr as well as $^{40}Ar/^{39}Ar$ ages of phengitic white mica of the cover rocks record an Alpine metamorphic event at about 80 Ma (Dallmeyer et al., 1996; Müller et al., 1999). These ages are supported by biotite Rb/Sr data of Grobgneiss rocks yielding ca. 72 Ma (Scharbert, 1990). Zircon and apatite fission track data suggest that the Grobgneiss rocks had

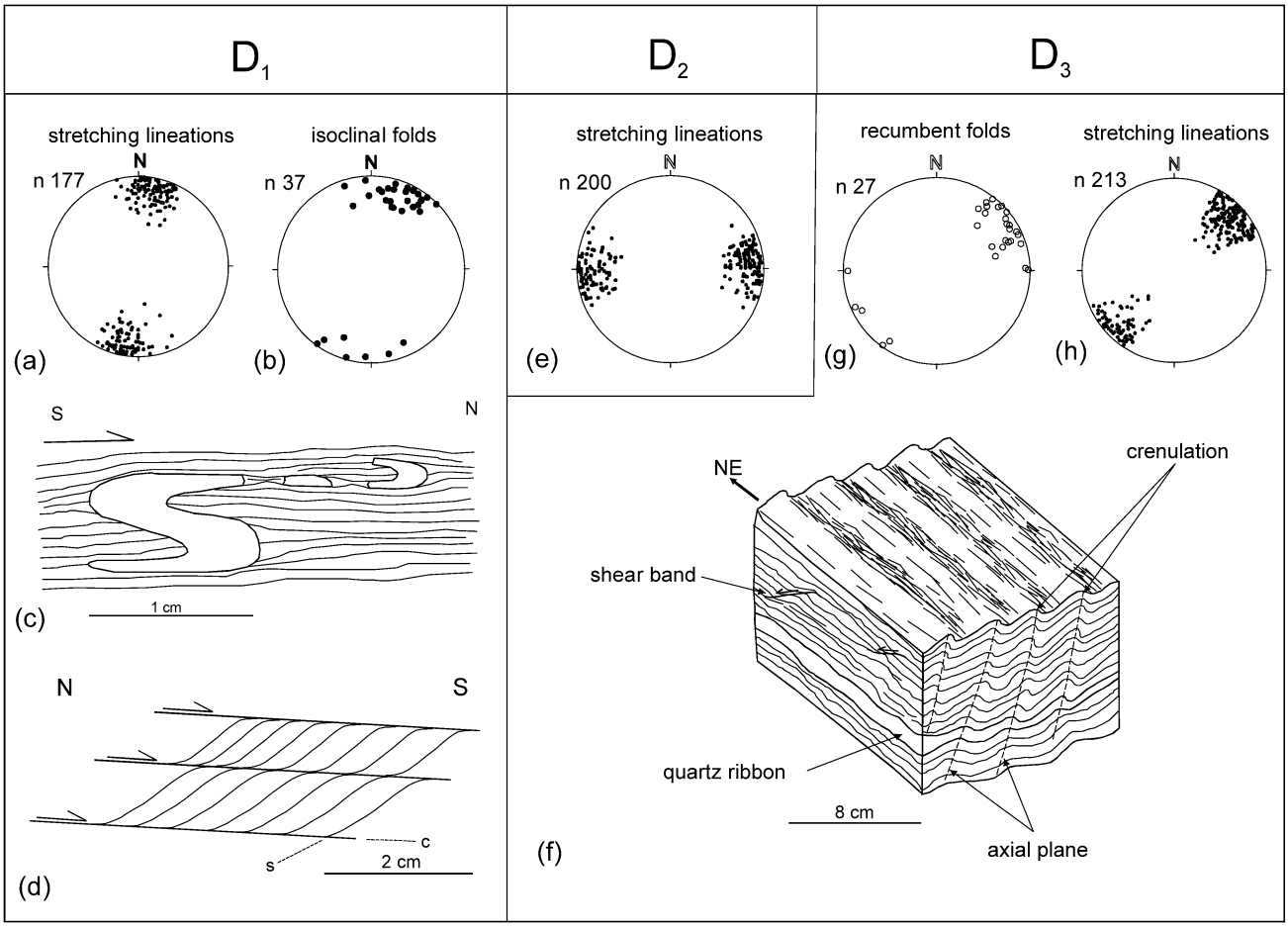

Fig. 3. Summary of structures measured (stereoplots) and observed (drawings) in the field for deformation phase D_1 (a–d), D_2 (e), and D_3 (f–h).

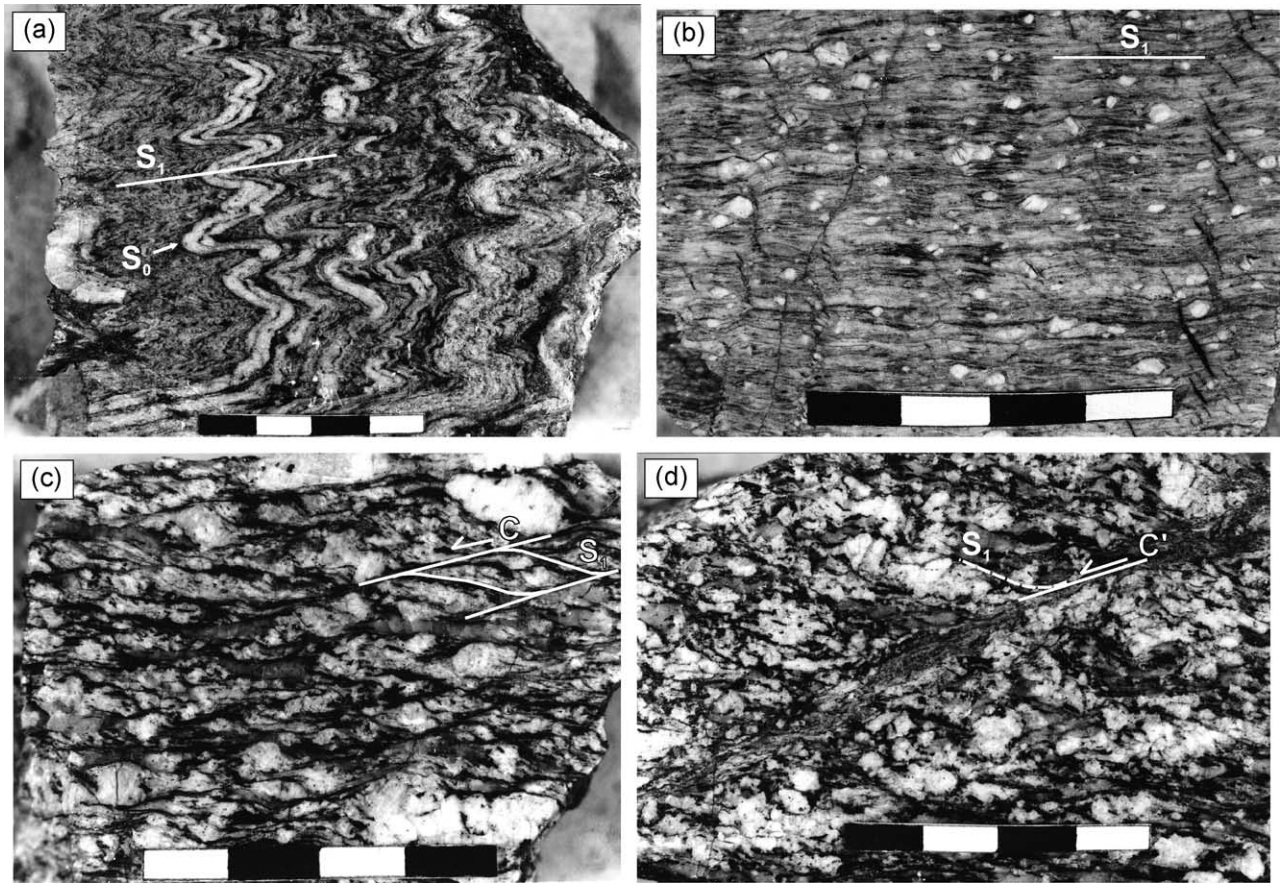

Fig. 4. Summary of representative structures for D_1 (a, b), D_2 (c) and D_3 (d) deformation phases. (a) Isoclinal folds in phyllonite of the Kirchberg nappe. The sample was taken at the hinge area of the fold nappe to the north of the Scheiblingkirchen Window. The axes of the folds trend NNE–SSW (Fig. 3a). (b) Ultramylonite from the Kirchberg nappe. Sample location: ca. 4 km to the northeast of the village Thomasberg. Note the strong reduction in grain size. The D_1 mylonite was overprinted by D_3 tension gashes. (c) *C–S* structure within a metagranite of the Kirchberg nappe with sinistral (top-to-the-W) sense of shear. Sample location: ca. 2.5 km to the east of the village Bromberg. (d) Low temperature shear band (C') in metagranite of the Kirchberg nappe. Sample location: at the northern border of the village Thomasberg. Scale bar division for all samples is 1 cm.

already reached a near surface position during the Late Cretaceous (Dunkl, 1992).

3. Structural analysis

Structures were mapped at a total of 417 stations all over the study area. A relative succession of deformation events could be established on the basis of overprinting criteria. Sets of structures belonging to the same deformation phase have been correlated within the study area using their style, geometry and orientation as distinguishing marks (e.g. Williams, 1985). Shear sense indicators like shear bands, *C–S* fabrics or asymmetric pressure shadows were used to obtain information on the kinematics of the deformation phases (for a review see Hanmer and Passchier, 1991) on the macroscopic as well as microscopic scale. Thin sections, prepared for kinematic and textural analysis were cut parallel to the stretching lineation and perpendicular to the foliation plane (*XZ* plane).

Lattice preferred orientations were studied in a total of 60 samples using U-stage as well as X-ray goniometry techniques at the Karl Franzens University in Graz (Austria). X-ray goniometry was performed on a Siemens D 5000 apparatus. The obtained raw data were recalculated with the software package of Siemens (DIFFRAC-AT V3.2) and intensities were corrected using the harmonic method of Bunge (1985).

3.1. Map- to meso-scale structures

As already mentioned in Section 2, Alpine tectonics caused a strong retrograde overprint of Variscan metamorphic fabrics. Deformation associated with the Alpine overprint was pervasive in the study area largely erasing pre-Alpine metamorphic and structural fabrics. Remnants of pre-Alpine metamorphic assemblages comprise garnet and hornblende found in a few samples only.

3.1.1. Deformation phase D_1

Northward closure of the flat-lying Kirchberg fold nappe is evident in map and cross-sectional views from an E–W

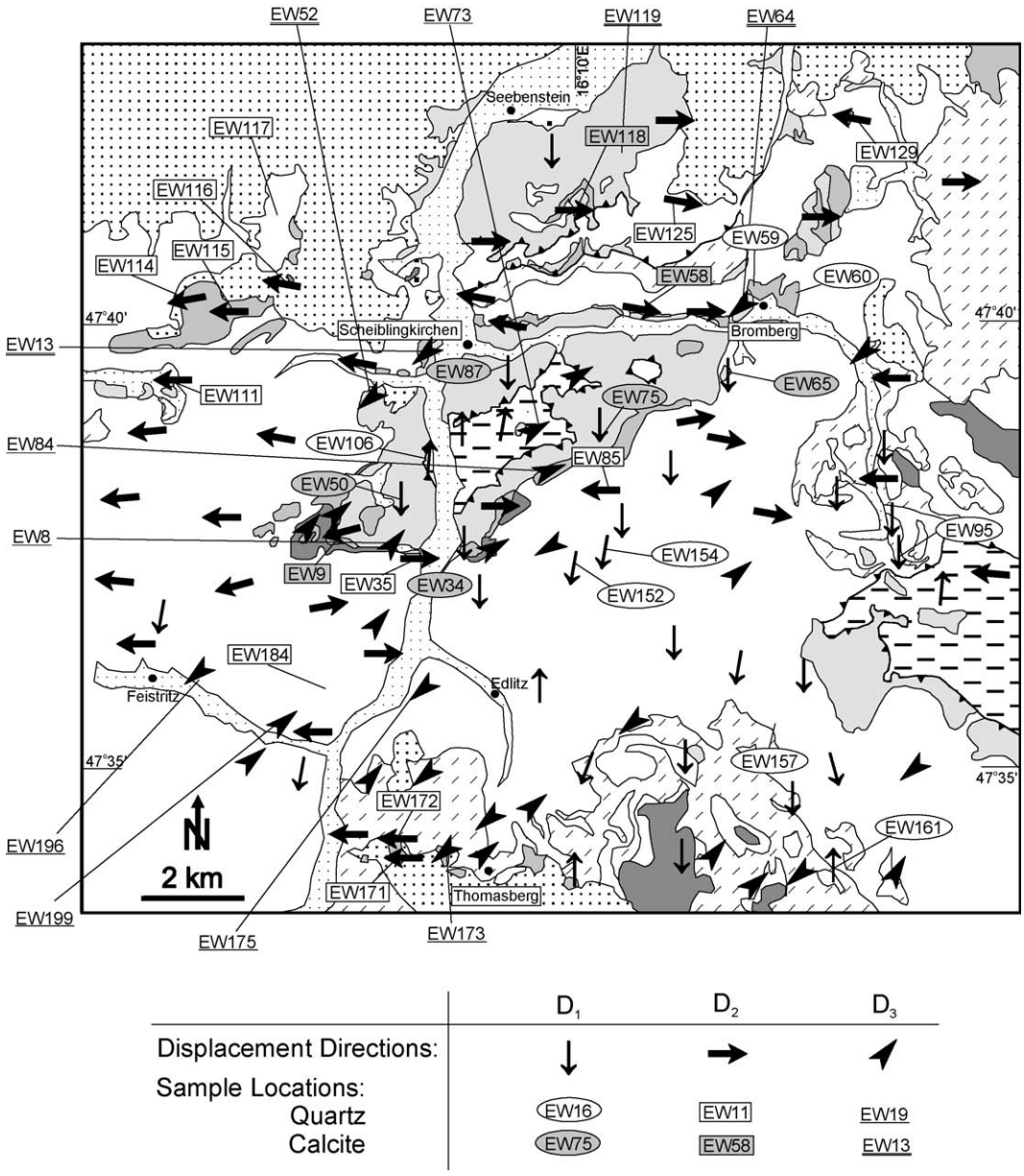

Fig. 5. Transport directions displayed for various deformation events are based on outcrop-scale and microstructural observations and texture analysis. The locations of samples used for texture analysis (Section 3.3) are shown. Legend for geologic units as in Fig. 2.

aligned stripe of metagranites to the north of the village Scheiblingkirchen that indicates the position of the fold hinge (Fig. 2). Such orientation of the fold nappe suggests northward thrust motion and overturning. At outcrop-scale the most prominent D_1 structure in all lithologies is a penetrative foliation (S_1), which contains a N to NNE-trending stretching lineation (L_1) (Fig. 3a). Locally within quartzites and scarce amphibolites, a mineral lineation defined by tourmaline and newly grown green hornblende can be observed, which is oriented sub-parallel to L_1. The relationship of S_1 to a pre-existing foliation, here referred to as S_0, is only observed in the fold hinge area. There, intense isoclinal folding of S_0-surfaces around subhorizontal axes (Fig. 3b) was associated with the formation of S_1 foliation planes representing an axial plane foliation to the isoclinal folds on hand specimen-scale (Fig. 4a), as well as to the recumbent fold nappe on a larger scale. This relationship emphasises the genetic link between S_1 and the fold nappe formation that is consistent with the occurrence of L_1 at and close to the nappe boundary. The present-day orientation of S_1, however, reflects the influence of multiple deformation phases superimposed on D_1 (see below).

D_1 structures within the phyllites and phyllonites of the Wechsel nappe close to or at the nappe boundary are shear bands or boudinaged isoclinal recumbent folds (Fig. 3c) indicating top-to-the-N displacement (Fig. 5). In contrast, the dominant transport direction in the Kirchberg nappe is top-to-the-S as inferred from *C*–*S* structures (Fig. 3d), shear

bands and σ-clasts denoting that these structures were formed within the overturned limb of the fold nappe (Fig. 5). Sporadically observed top-to-the-N shear structures could either be related to the high flattening component involved in fold nappe formation, allowing material to flow in the opposite direction too, or could simply represent erosional remnants of the upright limb. In general, however, coaxial deformation structures like symmetric pressure shadows around feldspar clasts dominate.

In the study area a southward increase of strain can be observed such that D_1 structures are less frequent in the area of the fold hinge relative to the limb areas (Fig. 5) where the rocks are more intensely sheared. Strain concentration caused the formation of shear zones a few meters thick, marked by a very close spacing of the foliation planes. Within these shear zones that contain a N-trending stretching lineation too, a distinct grain-size reduction leads to the development of ultra-mylonites, as shown in Fig. 4b.

Altogether D_1 structures suggest that they have been formed during the formation and emplacement of the Kirchberg nappe over the Wechsel nappe.

3.1.2. Deformation phase D_2

D_2 structures are restricted to outcrop-scale ductile shear zones, which are oriented parallel or sub-parallel to S_1. A D_2 related mylonitic foliation and a flat sub-horizontal to gently dipping, E–W trending stretching lineation (Fig. 3e) are defined by the growth and alignment of large white micas (up to 5 mm). Prominent features of D_2 are the formation of quartz and mica-rich mylonites (leucophyllites) within ductile shear zones of the metagranites. Metagranites containing a D_1 (N–S) oriented stretching lineation are successively replaced by leucophyllites within ca. half-meter-thick zones. Feldspar and biotite are gradually replaced by quartz, white mica and chlorite. Extensional crenulation cleavages (ecc structures) within the leucophyllites, interpreted as late stage D_2 features, show normal displacement. This is confirmed by *C–S* structures (Fig. 4c), asymmetric pressure shadows around porphyroclasts and shear bands, found within mylonites of the metagranites as well as phyllonites and rocks of the cover series of the Kirchberg nappe. The sense of displacement, deduced from the above named indicators, is variable (top-to-the-E or reverse). Interestingly, dominant top-to-the-W displacement directions have been found west of the Scheiblingkirchen Window, whereas dominant top-to-the-E displacement is observed east of the Scheiblingkirchen Window (Fig. 5) emphasizing overall coaxial deformation conditions.

3.1.3. Deformation phase D_3

In this section we describe structures that have been formed in the course of this deformation event (D_{3a}) as well as those that formed in response to it (D_{3b}).

D_1 and D_2 structures are overprinted by NW–SE contraction related structures (D_{3a}). Large-scale folding (F_{3a}) of the penetrative and mylonitic foliations resulted in the formation of the antiformal Scheiblingkirchen Window. The large-scale upright and open folds have a wavelength in the order of 6 km (Fig. 2). Related outcrop-scale folds with wavelengths of some meters show NE–SW trending fold axes, commonly plunging slightly towards NE (Fig. 2). Within phyllites of the Wechsel nappe a centimeter-scale crenulation (Fig. 3f) is observed, also showing NE–SW trending fold axes. An opposite vergence of outcrop-scale folds can be observed on both sites of the Scheiblingkirchen anticline (Fig. 2). Furthermore, shortening caused backthrusting to the north of the Scheiblingkirchen Window along the interface of the crystalline basement and the cover series of the Kirchberg nappe (Fig. 2). A distinct change in the dip angle from ca. 30–40° in the basement to ca. 50–60° in the backthrusted cover can be recognized in outcrops (Fig. 2).

Antiformal doming of the Scheiblingkirchen Window was followed by vertical flattening (D_{3b}) stretching the nappe pile in a NE–SW direction. Unlike D_1, D_{3b} outcrop-scale recumbent folds (F_{3b}) are open and display NE–SW trending fold axes (Fig. 3g). A related flat-lying axial plane foliation (S_{3b}) contains a weakly developed stretching lineation (L_{3b}), defined by quartz and fine-grained white mica, which trends parallel to the F_{3b}-fold-axes (Fig. 3h).

In general, D_3 shear structures like narrow shear bands (Figs. 3f and 4d) or extensional crenulation cleavages, which are typical for this deformation event, are found within all lithologies and suggest low-temperature deformation conditions. Cataclasis of feldspar and the segregation of quartz into ribbons support this observation. Again, alternating shear directions (Fig. 5) points to overall coaxial deformation conditions. Yet it remains unclear whether shear bands that emphasize extensional deformation orthogonal to the shortening direction (Fig. 3f) are contemporaneous with D_{3a} or slightly younger (D_{3b}).

Further evidence for D_{3b} flattening is given by a pressure solution cleavage, found in the Triassic carbonates, which is sub-parallel to the penetrative foliation S_1, and by steeply NE- or SW-dipping extensional veins, which are filled with calcite or quartz, dependent on host rock lithology.

Subsequent to D_3 the study area has been refolded around NW-trending fold axes (Fig. 2), referred to as 'Querfaltung' by Riedmüller (1967), and was subject to Neogene brittle deformation that was synchronous with ductile extension of lower plate Penninic rocks (Ratschbacher et al., 1990).

3.2. Microstructures

Microstructures are described following the chronology used in the previous section. The most prominent microstructural features of the different deformation stages are illustrated in Fig. 6. Special attention is paid to the minerals quartz and calcite, which were used for texture analysis (Section 3.3). All features and their orientation with

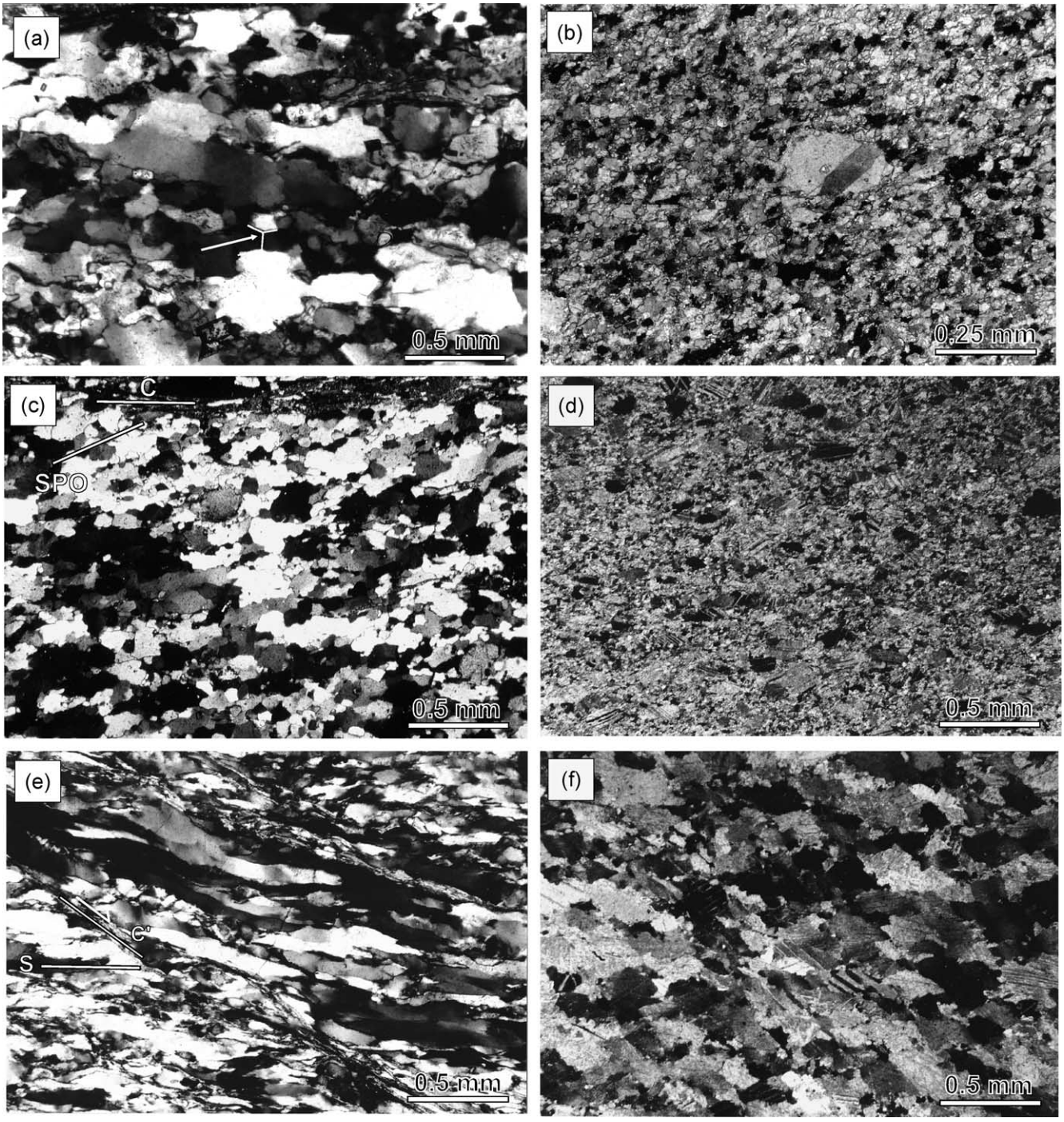

Fig. 6. Representative microstructures for D_1 (a, b), D_2 (c, d), and D_3 (e, f). The sample locations are shown in Fig. 5. (a) Sample EW106 from the Wechsel nappe close to the nappe boundary. The arrow points to triple point junction within a quartz-rich layer (enhanced by the white lines). (b) Core–mantle structure within a calcite ultramylonite (sample EW75). Note the relatively broad twin lamella within the host grain. (c) Dynamically recrystallized quartzite (EW172). The top part of the photograph shows a shape preferred orientation (SPO) of quartz grains aligned oblique to the bounding shear planes. (d) D_2 microstructure of a calcite mylonite (EW58). (e) Low-temperature microstructure of a quartzite (EW84) showing extremely flattened grains and a low degree of recrystallization. C' shear bands indicate dextral sense of shear. (f) D_3 microstructure of a calcite marble (EW13). Note the increased grain size and the distinctly higher abundance of twins compared with (b) and (d).

respect to a geologic frame (*XZ* plane) observed with the optical microscope (e.g. grain–grain relationships, grain boundaries, subgrains or kinematic indicators) are referred to as microstructure.

3.2.1. D_1-microstrutures

D_1 microstructures of phyllites of the Wechsel nappe and phyllites, micaschists and phyllonites of the Kirchberg nappe are characterized by a distinct segregation into

quartz–feldspar and sheet-silicate-rich layers. Within the quartz-rich layers, quartz displays a bimodal grain-size distribution. Large porphyroclasts of quartz are approximately equidimensional or slightly elongated with mean aspect ratios of 2:1 (Fig. 6a). The grain boundaries are angular, slightly curved or bulged. The porphyroclasts typically display an undulose extinction and subgrain formation is common. All these features together point to dynamic recrystallization processes during D_1. A few samples show dominantly straight grain boundaries and extinction, typical for static recrystallization, which could be interpreted in terms of late stage D_1 features, formed when deformation ceased.

Recrystallized grains are isometric in shape, smaller than 6 μm and form high angle boundaries with the host-grains. Their straight or slightly curved grain boundaries tend to form triple-point junctions (Fig. 6a). The quartz microstructure as a whole, however, suggests that dislocation climb was the dominant deformation mechanism. Ultramylonites, developed in metagranites also show a bimodal grain size distribution of quartz. Large grains are highly strained (length–width ratio of ca. 6:1) and surrounded by small, dynamically recrystallized grains to form core–mantle structures. Feldspar typically displays an eye-like shape. Fine-grained quartz and feldspar recrystallize within dominantly symmetric pressure shadows of the porphyroclasts.

The characteristics of D_1 ultramylonites from marbles of the Kirchberg nappe are shown Fig. 6b. The microstructure shows a high degree of recrystallization. A very fine-grained, recrystallized calcite matrix surrounds relics of twinned host grains. The grain boundaries of the matrix grains are straight, sometimes bulged and the equidimensional grains are smaller than 6 μm in diameter. Twinning of these grains is only observed in grains larger than 3 μm. Twins of the old relics are sometimes lensoid shaped, a feature known from laboratory experiments above ca. 400 °C (e.g. Rowe and Rutter, 1990). The small grain size, the equidimensional shape of the grains, the mostly straight grain boundaries and the absence of a shape preferred orientation points to the possibility that grain boundary sliding may have played a role beside dislocation creep as operating deformation mechanism (see also Schmid et al., 1987; Passchier and Trouw, 1998). In contrast *C–S* mylonites have larger grain sizes, elongated grains and irregular grain boundaries indicating that dislocation creep is the dominant deformation mechanism.

3.2.2. D_2-microstructures

In contrast to D_1 microstructures, no ultramylonites were formed during D_2. Instead the growth of coarse-grained white mica, which defines a mylonitic foliation indicate that deformation temperatures were approximately as high as during D_1. Shear bands, ecc structures, and rotated mineral clasts (feldspar, garnet) are the most frequent shear sense indicators. Together with the E–W trending stretching lineation they suggest E–W extension. In some samples a noncoaxial component can be deduced from the shape preferred orientation of quartz grains as shown in Fig. 6c. Core–mantle structures are only found in *C–S* mylonites of the metagranites. Similar to D_1 microstructures, quartzites of the cover series show a bimodal grain-size distribution, but grain boundaries are dominantly serrated or bulged (Fig. 6c). Subgrain formation is common within host grains and less frequent in recrystallized grains. Altogether, the microstructural features mentioned above suggest that dynamic recrystallization by grain-boundary migration was the most important recrystallization process in this case (Fig. 6c) driven by dislocation creep. It is important to note that lensoid shaped feldspar clasts within the phyllonites or the Alpine Verrucano Formation of the Kirchberg nappe show ductile deformation features like an undulose extinction, too.

Similar to quartz, calcite also shows signs of dislocation creep expressed by dynamic recrystallization features like bulged grain boundaries (Fig. 6d). Additionally, twinning seems to be more important during D_2 compared with D_1.

3.2.3. D_3-microstructures

D_3 microstructures differ distinctly from D_1 and D_2 microstructures described above. We interpret them to represent the last ductile increment associated with the formation of the Scheiblingkirchen Window. Discrete shear bands and C' structures show dominant top-to-the-NE displacement (Fig. 6e). Fine-grained white mica recrystallizes along the shear bands and also defines an extensional crenulation cleavage. The sense of shear is also deduced from the shape preferred orientation of quartz within quartz layers in phyllites of the Wechsel nappe as well as phyllonites of the Kirchberg nappe. Typically, quartz aggregates are aligned obliquely (40–60°) to the shear planes, defined by sheet silicates. Cracks within feldspar clasts are filled with quartz having equidimensional or slightly elongated grain-shapes. Undulose extinction of the quartz grains point to a syn-deformational filling of the cracks. Intense deformation within quartzites or quartz-rich aggregates is documented by extremely elongated quartz grains (aspect ratios up to 8:1, Fig. 6e). Subgrain formation is common and grain boundaries are serrated or bulged. Small dynamically recrystallized grains are less frequent than in D_1 or D_2 microstructures and large quartz grains often show deformation lamellae, indicating low-temperature deformation conditions.

Deformation by twinning becomes more important in carbonates (Fig. 6f) and seems to dominate over creep processes. Host grain- as well as twin-boundaries are serrated pointing to deformation temperatures above ca. 250 °C (Burkhard, 1993). However, the presence of narrow twins, indicative for low deformation temperatures (Burkhard, 1993), may be a late stage feature of D_3. Bending of the crystal lattice is evidenced by an undulose extinction. Generally one dominant set of twins developed, and as in

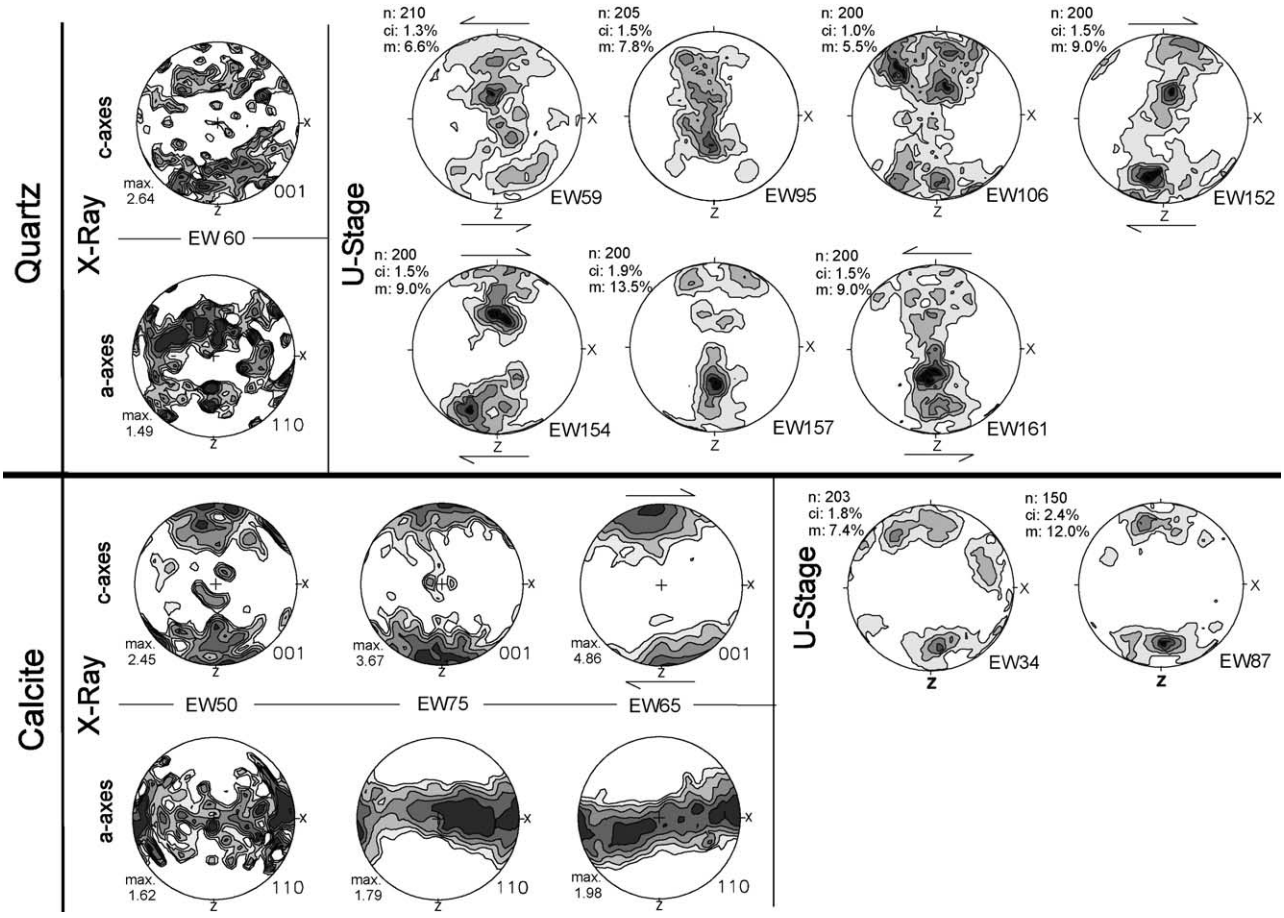

Fig. 7. Summary of D_1 quartz and calcite textures. [*c*] (001 surfaces) and ⟨*a*⟩ (110 surfaces) axes measured with the X-ray texture goniometer are contoured logarithmically with the maxima as noted beside the plots. Both, X-ray and U-stage data are displayed as equal area lower hemisphere projections. Counting statistics are displayed at the left upper corner of the corresponding stereoplot; *n* is number of measured grains, *ci* is contour interval in percent, and *m* gives the number of points in the maximum in %. Sample locations are displayed in Fig. 5.

the quartz, the amount of recrystallized grains is distinctly less than in D_1 and D_2 microstructures. From all the above named features we infer that twinning and dislocation glide dominates over creep processes during D_3.

3.3. Texture analysis

Lattice preferred orientations of quartz and calcite are presented according to the sequence of events described in the previous chapters. Since the textures of the Wechsel and Kirchberg nappes do not differ significantly, they are described together. We use texture analyses to infer the operative slip systems, the strain symmetry, the sense of shear, and the strain geometry. The latter has to be seen as a first order qualitative description since supporting strain measurements are not available.

3.3.1. D_1-textures

D_1 quartz *c*-axis patterns (Fig. 7) display pronounced maxima at the position of the rhomb planes suggesting that glide on these planes parallel to ⟨*a*⟩ dominated over prism and basal ⟨*a*⟩ slip. The lattice preferred orientation resembles (partly incomplete) crossed girdles that may be developed as type I, i.e. small circles around *Z* are connected by a single girdle through *Y* (EW106), or type II, i.e. two girdles around *X* joining at *Y*, crossed girdles (EW157, EW161) according to the classification of Lister (1977). The asymmetry of some textures (with respect to the *XZ* plane), as illustrated by sample EW152, points to a non-coaxial strain path. However, the occurrence of small girdles around *Z* seems to reflect an important contribution of a flattening component. Such strain geometries, as represented by sample EW106 taken close to the nappe boundary (corresponding microstructure is shown in Fig. 6a), are expected in relation to fold nappe formation. Although weakly defined, the crystallographic preferred orientation of *c*- and ⟨*a*⟩-axes of sample EW60 from the fold hinge area support flattening strain conditions.

Interestingly, the *c*-axis pattern from a local shear zone within the metagranite (sample EW95) differs such that glide was confined to the prism and rhomb planes, which is thought to be indicative for higher deformation temperatures (e.g. Law, 1990). Similar quartz *c*-axes pattern have been described by Berthé et al. (1979) for amphibolite grade

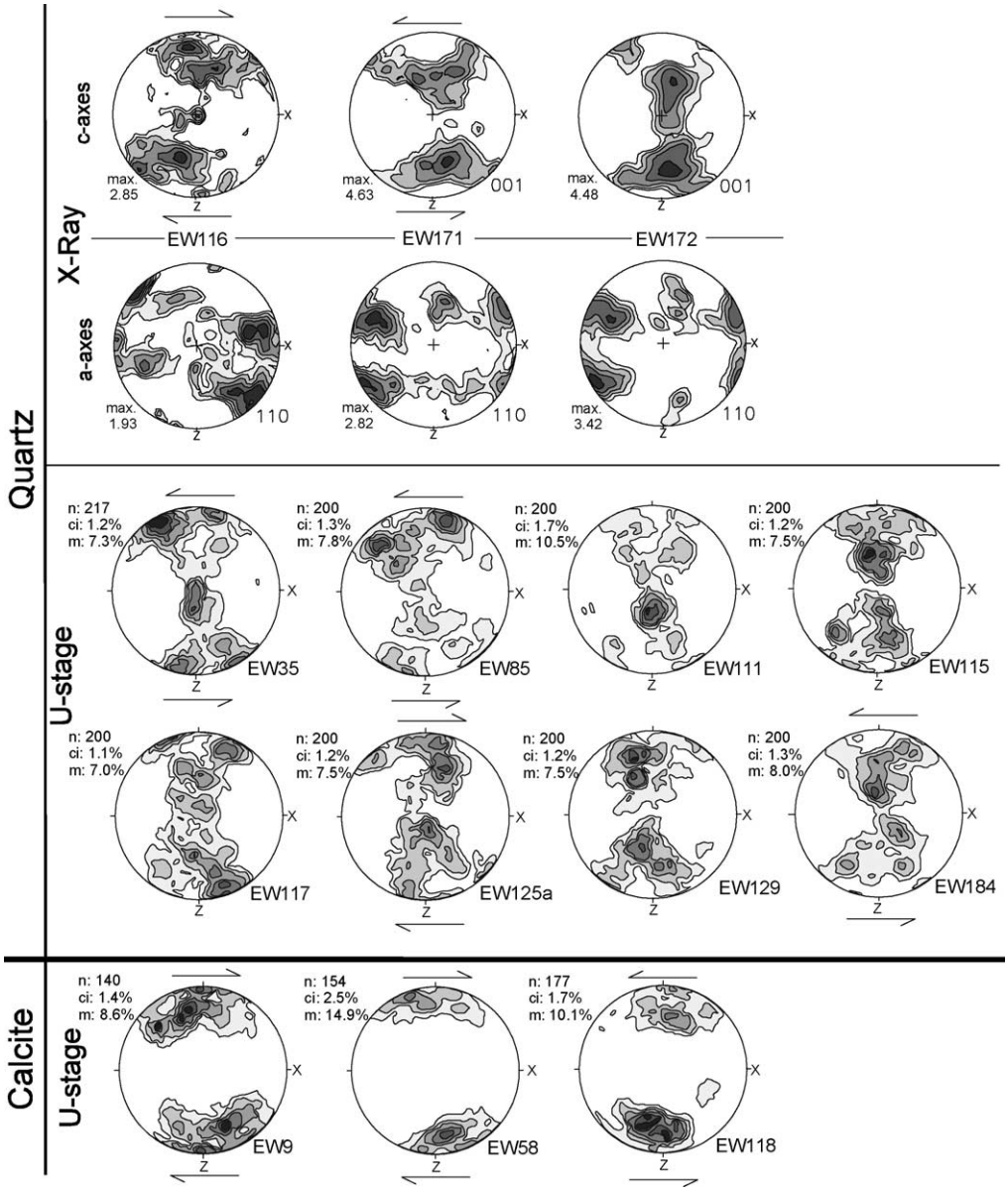

Fig. 8. Summary of D_2 quartz and calcite textures. Representation and abbreviations as in Fig. 7.

rocks from the South Armorican shear zone. However, the cause for the apparent temperature rise recorded by sample EW95 is still unclear.

Calcite *c*-axis distributions of very fine-grained samples (see Fig. 6b) show a moderate lattice preferred orientation with maxima at or close to *Z* (Fig. 7). The corresponding ⟨*a*⟩-axes (Fig. 7) are aligned in single girdles parallel to the *XY* plane of the finite strain ellipsoid with submaxima close to *Y* (EW75) or *X* (EW50, EW65). Slight asymmetries of the textures with respect to the reference frame (*XZ* plane) indicate a contribution of a noncoaxial shear component. The texture, however, is comparable with textures known from rock experiments and numerical model studies under low temperature conditions (e.g. Wenk et al., 1987).

3.3.2. D_2-textures

The dominant D_2-related quartz lattice preferred orientations (Fig. 8) represent crossed girdles of type I (e.g. EW172, EW85) or type II (e.g. EW35) or small circles around *Z* (e.g. EW116, EW171). Correspondingly, the *a*-axes form point maxima close to *X* (EW172, for corresponding microstructure see Fig. 6c) or small circles around *Z* with a high opening angle (EW116 and EW171). In most of the textures distinct submaxima at rhomb position are observed. Additionally, slip along ⟨*a*⟩ on the basal and prism planes was important during D_2. Similar to D_1 textures a non-coaxial component of shear could be deduced on the basis of asymmetric *c*- and ⟨*a*⟩-axis patterns. Our D_2 quartz textures show many similarities to *c*-axes pattern

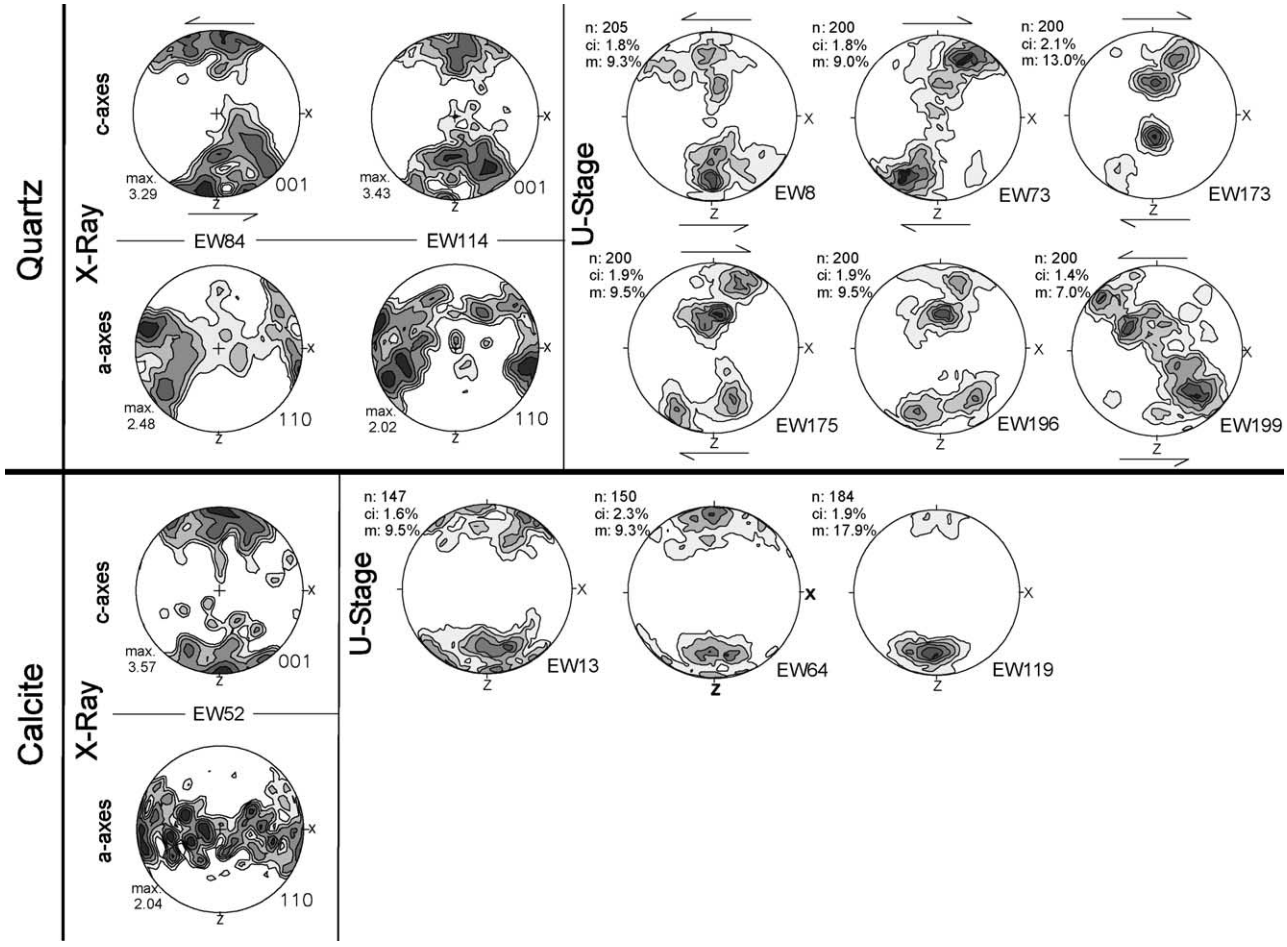

Fig. 9. Summary of D_3 quartz and calcite textures. Representation and abbreviations as in Fig. 7.

compiled by Price (1985) for plane strain and flattening strain geometries.

Similar to D_1 textures, calcite *c*-axis maxima group around *Z* (Fig. 8). Slip on the basal and rhomb planes is thought to accommodate most of the deformation, although twinning becomes more important relative to D_1.

The strain geometry inferred from the lattice preferred orientations is in agreement with structural observations that point to vertical flattening and E–W extension post-dating the stacking event.

Furthermore, there is no profound difference regarding the active slip systems during D_1 and D_2 suggesting that temperature conditions did not change significantly.

3.3.3. D_3-textures

D_3 quartz textures often represent a composite texture comprising pre-D_3 and D_3 features. The last increment of ductile deformation is frequently expressed by a shape preferred orientation of quartz ribbons (see also Section 3.2.3), which coincides with a lattice preferred orientation shown in Fig. 9. *C*-axes from these ribbons indicate that slip on the basal planes parallel to ⟨*a*⟩ was the dominant glide system during D_3 (e.g. EW73, EW84; Fig. 9). Quartz *c*-axes outside the domains with shape preferred orientation underline the importance of glide on the rombs prior to D_3 (e.g. EW173 or EW175; Fig. 9). The relative importance of glide on the basal planes with respect to glide on the prism planes points to lower deformation temperatures during D_3 compared with D_1 or D_2. Textures, which can entirely be related to D_3, based on microstructural observations, represent incomplete type II crossed girdles (EW84) or single girdles (EW199). Especially the texture of EW84 that was deduced from a sample with extremely flattened grains (Fig. 6e) provides valuable information on the strain geometry during D_3. In this case, the ⟨*a*⟩-axes form small circles around *X*, what can be expected under constrictional strain conditions. Unlike D_1 and D_2 textures, nearly all D_3 lattice preferred orientations suggest an important component of non-coaxial shear.

In contrast to quartz, D_3 calcite textures (Fig. 9) do not differ significantly from those of D_1 or D_2 although a gradual change from dominant intra-crystalline glide (D_1, D_2) to twinning (D_3) can be inferred from the microstructure. The *c*-axes of the host grains cluster around the maximum shortening direction *Z* (Fig. 9). Similar to D_1

textures ⟨*a*⟩-axis tend to form a single girdle parallel to the stretching direction (*X*).

4. Discussion

In this section we put the new data, described in the previous sections, in the context of the Cretaceous tectonic evolution of the Eastern Alps.

4.1. Nappe stacking and the relationship of metamorphism and deformation

Accretion of the Lower Austroalpine unit, which is thought to represent the northern passive margin of the Austroalpine microcontinent, by underthrusting underneath the already stacked Middle and Upper Austroalpine nappe complexes occurred at ca. 80 Ma (e.g. Dallmeyer et al., 1996, 1998; Müller et al., 1999). The stacking related metamorphism reached lower greenschist facies conditions within the Wechsel nappe and lower greenschist (in the N) to lower amphibolite facies (in the S) metamorphism within the Kirchberg nappe (e.g. Dallmeyer et al., 1996; Frey et al., 1999). Within the crystalline basement this metamorphism caused an intense retrogression of Variscan fabrics, whereas the cover sequences display a prograde metamorphic path. According to Müller et al. (1999) underthrusting of the Lower Austroalpine Unit occurred by top-to-the-W to NW shearing. Subsequent out-of-sequence thrusting caused the emplacement of the higher grade Kirchberg nappe onto the lower grade Wechsel nappe (e.g. Dallmeyer et al., 1998) corresponding to the main deformation phase D_1 in our study area. Such relationships suggest that D_1 intra-Lower Austroalpine nappe stacking is related to the decompression path of the Kirchberg nappe. Decompression most likely did not occur under decreasing temperatures since no higher-grade mineral assemblages of previous Alpine deformation events (underthrusting of Lower Austroalpine Unit), are preserved in our study area. D_1 temperature conditions, however, were sufficiently high for the syn-kinematic growth and alignment of small garnets and green amphibole within micaschists and lenses of amphibolite in southernmost parts of the study area. Top-to-the-N movement, as inferred from fold–nappe geometry and kinematic indicators on various scales, points to a change in the maximum shortening direction from E–W to SE–NW during the underthrusting stage to ca. N–S during D_1 (Fig. 10a). Such contraction directions have also been deduced for the exhumation and cooling history of Middle Austroalpine units farther to the west (Neubauer et al., 1995) and the westernmost Austroalpine plate margin (Ring et al., 1988). On the scale of the orogen, deformation has been partitioned into thrusting at lower structural levels (Lower Austroalpine units), strike-slip and folding dominated deformation at intermediate structural levels (Middle Austroalpine units), and extensional deformation at highest structural levels (Upper Austroalpine units) leading to the extensional unroofing of the orogen and associated basin formation (e.g. Willingshofer et al., 1999b; Neubauer et al., 2000). Similar relationships have been observed for the French Variscan Belt by Aerden and Malavieille (1999) where extension of the orogen is coeval with basal accretion of thrust sheets and fold nappe formation. We suspect that the shift to top-to-the-N kinematics is related to the change of the African plate motion from southeastward to northeastward with respect to Europe (Dewey et al., 1989). A time constraint for the nappe emplacement is given by $^{40}Ar/^{39}Ar$ age data of muscovite from the base of the Kirchberg nappe yielding 71 Ma (e.g. Dallmeyer et al., 1998). This age is interpreted to represent post-metamorphic cooling (Dallmeyer et al., 1998). Since cover sequences of the Wechsel nappe are lacking in the area of the Scheiblingkirchen Window we assume that they have been cut out during out-of-sequence thrusting. Fold nappe formation probably nucleated at a lateral discontinuity that might have been geometrically (ramp-type structure in Fig. 10a) or rheologically controlled, resembling in any case an obstacle during continuous shortening. Subsequent northward motion of the large-scale recumbent fold was associated with the formation of S_1, a penetrative axial plane foliation to the fold nappe (Fig. 10a). Quartz microstructures (straight, slightly curved or bulged grain boundaries) and textures (mainly rhomb and prism ⟨*a*⟩ slip) are in agreement with temperature conditions deduced from isotope geology pointing to low temperature deformation during D_1.

4.2. Decompression through E–W extension

The formation of narrow shear zones, parallel to S_1, with normal displacement during D_2 argues for a structurally controlled exhumation history of the Scheiblingkirchen Window. Similar features were reported throughout the Austroalpine nappe complex (e.g. Neubauer et al., 1995; Froitzheim et al., 1997; Koroknai et al., 1999; Fügenschuh et al., 2000). Unlike Müller et al. (1999) who relate the top-to-the-W shearing west of the Scheiblingkirchen Window to the stacking event, we interpret these structures as indication of E–W extension post-dating the emplacement of the Kirchberg onto the Wechsel nappe based on the following considerations: (1) outcrop-scale shear zones with E–W trending stretching lineations occur within rocks already deformed during D_1, and (2) alternating shear directions west and east of the Scheiblingkirchen Window (see Fig. 5). Such a displacement pattern suggests a geometrical control on the flow direction inherited from D_1. Perhaps the ramp over which the Kirchberg nappe was emplaced onto the Wechsel nappe acted as a 'flow divide'. Alternatively, the displacement pattern could resemble a progressive sequence of shear zone activations such as that known in relation to detachment systems (e.g. Lister and Davis, 1989).

Microstructural and texture analyses indicate that deformation temperatures (dominant rhomb ⟨*a*⟩ slip) did not

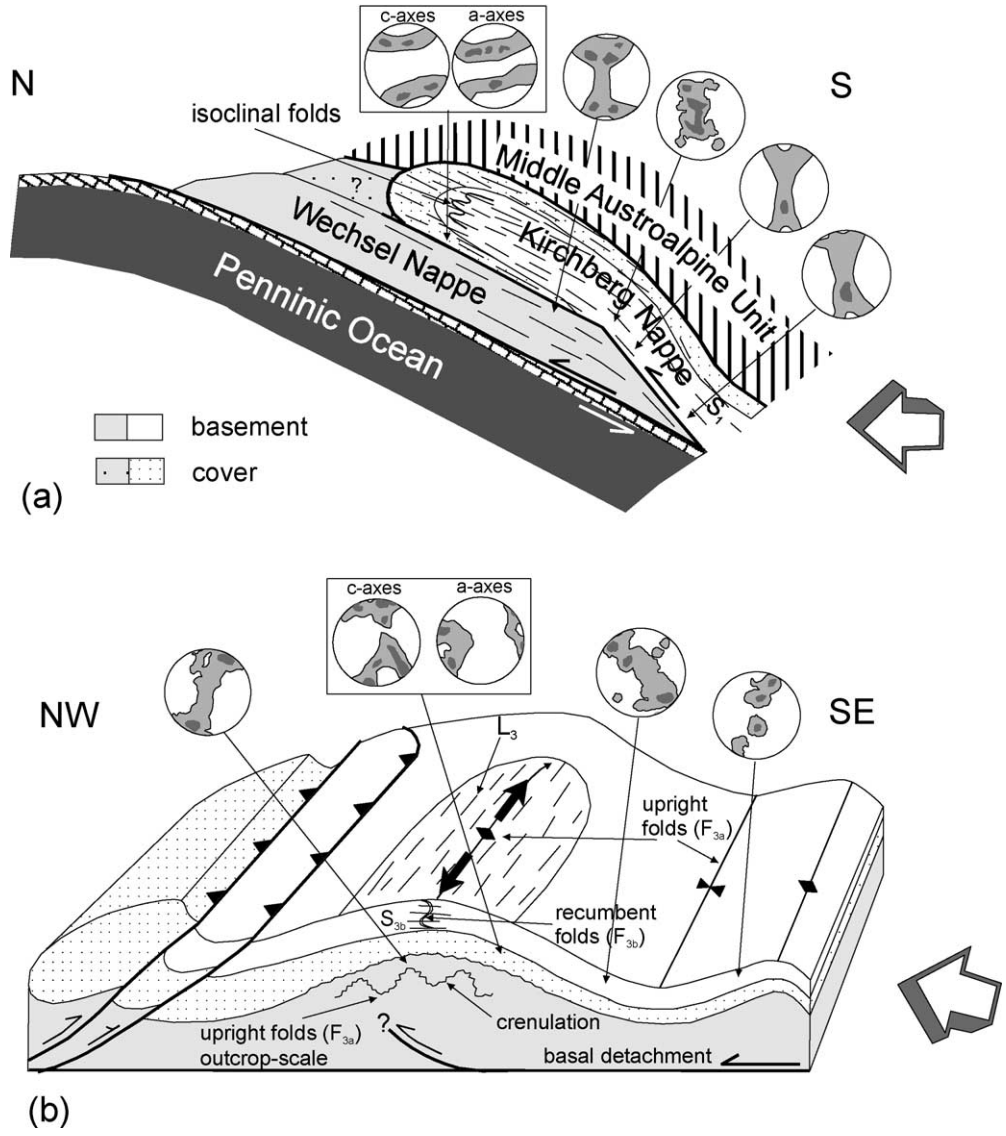

Fig. 10. Cartoons showing main stages of the Cretaceous tectonic evolution of the Scheiblingkirchen window and a summary of observed structures. Pole figures represent outlines of characteristic quartz *c*-axis patterns. (a) Fold nappe formation and related structures. (b) Antiformal doming of the Scheiblingkirchen Window. Signature as in (a).

change significantly with respect to D_1. We, therefore, interpret D_2 to represent a short-lived isothermal exhumation phase causing vertical shortening within the nappe pile. Such conditions are reflected in the quartz *c*-axes pattern pointing to an important flattening component (Fig. 8).

A peculiar D_2 feature is the formation of leucophyllites within metagranites. Chemical and petrological investigations of these rocks in the area of Sopron (Hungary), approximately 30 km to the east of our study area have shown that Mg-metasomatism drives leucophyllite formation (Demény et al., 1997). Mg-rich metamorphic fluids are derived from dehydration of simultaneously underthrusting sediments of the S-Penninic Ocean (Demény et al., 1997). The estimated *P–T* conditions of ca. 530 °C and 1.3 GPa (Demény et al., 1997) point to D_1 rather than to D_2 conditions. However, pressure conditions of this order are not confirmed within our study area by corresponding 'high pressure' mineral assemblages neither for D_1 nor for D_2.

4.3. Formation of the antiformal window

NW–SE directed contraction during D_3 resulted in large-scale folding of the area (Fig. 10b). D_3 is equivalent to the 'main folding phase' of Riedmüller (1967). Contraction was in our opinion predominantly accommodated: (1) by movements along a basal detachment, and (2) by back-thrusting to the north of the Scheiblingkirchen Window, already recognized by Fuchs (1990). Possibly antiformal doming was aided by the activation of a blind thrust departing from a basal detachment. A similar mechanism (movement along a blind thrust) is also thought to have played an important role during doming of the Sonnblick dome at the eastern

part of the Tauern Window (Kurz and Neubauer, 1996). Additionally, a certain amount of deformation was also taken up by smaller scale structures like outcrop-scale open folds or a crenulation of the penetrative foliation (S_1). Simple depth-to-detachment calculations, performed perpendicular to the shortening direction, using the 'excess area method' (Epard and Groshong, 1993) that relates the deformed area above a reference level to the amount of shortening gave displacements on the order of 1.24 km and a depth to the detachment of ca. 4 km (Willingshofer, 1995). A potential candidate for the basal detachment seems to be the interface between the Austroalpine and the Penninic units, the latter one actively underplating the Austroalpine nappe complex during the Late Cretaceous (e.g. Dallmeyer et al., 1998).

In response to shortening and antiformal doming, subsequent subvertical flattening resulted in the development of open recumbent folds (F3b) and an associated subhorizontal axial plane foliation, which contains a NE-trending stretching lineation (Fig. 10b). Structures on all scales record lower deformation temperatures relative to D_1 and D_2. Dynamic recrystallization processes are in their initial stage and basal $\langle a \rangle$ slip is the dominant glide system. Therefore, D_3 represents an important deformation event during the cooling history of the Lower Austroalpine unit at the eastern margin of the Eastern Alps. Apatite and zircon fission-track data (Dunkl, 1992) and thermal modelling (Willingshofer et al., 1999a) show that the Lower Austroalpine unit already kept a near surface position at the end of the Cretaceous to early Paleogene. This argues for a very rapid exhumation history of this crustal segment, mainly driven by a combination of contractional and extensional tectonic processes rather than erosion.

5. Conclusions

From our structural investigations we deduce that the main deformation phase in the area of the Scheiblingkirchen Window at the eastern margin of the Eastern Alps can be related to the emplacement of the Kirchberg fold nappe onto the Wechsel nappe. Out-of-sequence top-to-the-N overthrusting occurred during the decompression history of the Kirchberg nappe and marks the change from E–W to N–S shortening in the Eastern Alps during the Late Cretaceous; between ca. 80 and 70 Ma. Subsequent exhumation is controlled by the development of ductile shear zones within an E–W extensional regime under similar deformation temperatures. On the microstructural scale recrystallization processes play an important role during nappe emplacement as well as the subsequent exhumation phase during which glide on prism and rhomb planes seems to be more important than glide on the basal planes.

NW directed horizontal shortening resulted in antiformal doming of the Scheiblingkirchen Window and the activation of backthrusts to the north of the antiformal structure. Subsequent subvertical flattening caused stretching of the nappe pile parallel to the fold axis (NE–SW). Microstructural and texture analyses exhibit low temperature deformation features and allow the allocation of this deformation phase to the cooling history of the Scheiblingkirchen Window.

Acknowledgements

We appreciate assistance by Wolfgang Unzog during texture analyses with the X-ray goniometer at the University of Graz. Furthermore we wish to thank Harry Fritz and Walter Kurz for discussion on various related topics. Ernst Willingshofer acknowledges the assistance and pleasant company of Antoinette and Jakob during field work. The paper benefited from careful reviews by U. Ring and J.M. Tubia. This work was partly financed by the FWF P8652-GEO project and completed in the frame of NWO-ALW project 810.31.003. This is NSG publication No. 20011001.

References

Aerden, D.G.A.M., Malavieille, J., 1999. Origin of a large-scale fold nappe in the Montagne Noire, Variscan belt, France. Journal of Structural Geology 21, 1321–1333.

Berthé, D., Choukboune, P., Jegouzo, P., 1979. Orthogneiss, mylonite and non coaxial deformation of granites: the example of the South Armorican Shear Zone. Journal of Structural Geology 1, 31–42.

Bunge, H.J., 1985. Representation of preferred orientation. In: Wenk, H.R. (Ed.). Preferred Orientation in Deformed Metals and Rocks: an Introduction to Modern Texture Analyses. Academic Press, Orlando, pp. 73–108.

Burkhard, M., 1993. Calcite twins, their geometry, appearance and significance as stress-strain markers and indicators of tectonic regime: a review. Journal of Structural Geology 15, 355–368.

Dallmeyer, R.D., Neubauer, F., Handler, R., Fritz, H., Müller, W., Pana, D., Putis, M., 1996. Tectonothermal evolution of the internal Alps and Carpathians: evidence from $^{40}Ar/^{39}Ar$ mineral and whole-rock data. Eclogae Geologicae Helvetiae 89, 203–227.

Dallmeyer, R.D., Handler, R., Neubauer, F., Fritz, H., 1998. Sequence of thrusting within a thick-skinned tectonic wedge: evidence from $^{40}Ar/^{39}Ar$ and Rb–Sr ages from the Austroalpine nappe complex of the Eastern Alps. Journal of Geology 106, 71–86.

Demény, A., Sharp, Z.D., Pfeifer, H.-R., 1997. Mg-metasomatism and formation conditions of Mg–chlorite–muscovite–quartzphyllites (leucophyllites) of the Eastern Alps (W. Hungary) and their relations to Alpine whiteschists. Contributions to Mineralogy and Petrology 128, 247–260.

Dewey, J.F., Helman, M.L., Turco, E., Hutton, D.H.W., Knott, S.D., 1989. Kinematics of the western Mediterranean. In: Coward, M.P., Dietrich, D., Park, R.G. (Eds.), Alpine Tectonics. Geological Society Special Publications 45, pp. 265–284.

Dunkl, I., 1992. Final episodes of the cooling history of eastern termination of the Alps. ALCAPA-Field Guide, Graz, pp. 137–139.

Epard, J.L., Groshong, R.H., 1993. Excess area and depth to detachment. American Association of Petroleum Geologists, Bulletin 77, 1291–1302.

Faupl, P., Wagreich, M., 1996. Basin analysis of the Gosau Group of the Northern Calcareous Alps (Turonian-Eocene, Eastern Alps). In: Wessely, G., Liebl, W. (Eds.), Oil and Gas in Alpidic Thrust Belts

and Basins of Central and Eastern Europe. European Association of Geoscientists and Engineers Special Publication 5, pp. 127–135.

Faupl, P., Wagreich, M., 2000. Late Jurassic to Eocene Palaegeography and geodynamic evolution of the eastern Alps. Mitteilungen der Österreichischen Geologischen Gesellschaft 92, 79–94.

Frey, M., Desmons, J., Neubauer, F., 1999. Metamorphic map of the Alps. Schweizerische Mineralogische und Petrographische Mitteilungen, 79.

Frisch, W., 1979. Tectonic progratation and plate tectonic evolution of the Alps. Tectonophysics 60, 121–139.

Froitzheim, N., Conti, P., van Daalen, M., 1997. Late Cretaceous, synorogenic, low-angle normal faulting along the Schlinig fault (Switzerland, Italy, Austria) and its significance for the tectonics of the Eastern Alps. Tectonophysics 280, 267–293.

Fuchs, G., 1962. Neue tektonische Untersuchungen im Rosaliengebirge (Nö. Bgld.). Jahrbuch der Geologischen Bundesanstalt 105, 19–37.

Fuchs, G., 1990. Zum Bau des Unterostalpins im Bereich der Buckligen Welt. In: Koller, F. (Ed.), Wandertagung 1990 der Österreichischen Geologischen Gesellschaft in Bernstein, Exkursionsführer 13, pp. 28–29.

Fügenschuh, B., Mancktelow, N.S., Seward, D., 2000. Cretaceous to Neogene cooling and exhumation history of the Oetztal–Stubai basement complex, eastern Alps: a structural and fission track study. Tectonics 19, 905–918.

Hanmer, S., Passchier, C.W., 1991. Shear-sense indicators: a review. Geological Survey of Canada Paper 90-17, 1–72.

Koroknai, B., Neubauer, F., Genser, J., Topa, D., 1999. Metamorphic and tectonic evolution of Austroalpine units at the western margin of the Gurktal nappe complex, Eastern Alps. Schweizerische Mineralogische und Petrographische Mitteilungen 79, 277–295.

Krohe, A., 1987. Kinematics of Cretaceous nappe tectonics in the Austroalpine basement of the Koralpe region (eastern Austria). Tectonophysics 136, 171–196.

Kurz, W., Neubauer, F., 1996. Deformation partitioning and shear localization during the updoming of the Sonnblick area in the Tauern Window (Eastern Alps, Austria). Journal of Structural Geology 18, 1327–1343.

Law, R.D., 1990. Crystallographic fabrics: a selective review of their applications to research in structural geology. In: Knipe, R.J., Rutter, E.H., (Eds.), Deformation Mechanisms, Rheology and Tectonics. Geological Society Special Publication 54, pp. 335–352.

Lister, G.S., 1977. Discussion: crossed girdle *c*-axis fabrics in quartzites plastically deformed by plane strain- and progressive simple shear. Tectonophysics 39, 51–54.

Lister, G.S., Davis, G.A., 1989. The origin of metamorphic core complexes and detachment faults formed during Tertiary continental extension in the northern Colorado River region, USA. Journal of Structural Geology 11, 65–95.

Liu, Y., Genser, J., Handler, R., Friedl, G., Neubauer, F., 2001. $^{40}Ar/^{39}Ar$ muscovite ages from the Penninic-Austroalpine plate boundary, Eastern Alps. Tectonics 20, 526–547.

Müller, W., Dallmeyer, R.D., Neubauer, F., Thöni, M., 1999. Deformation-induced resetting of Rb/Sr and $^{40}Ar/^{39}Ar$ mineral systems in a low-grade, polymetamorphic terrane (Eastern Alps, Austria). Journal of the Geological Society London 156, 261–278.

Neubauer, F., Frisch, W., 1993. The Austroalpine metamorphic basement east of the Tauern Window. In: von Raumer, J.F., Neubauer, F. (Eds.). Pre-Mesozoic Geology in the Alps. Springer-Verlag, Berlin, pp. 515–536.

Neubauer, F., Müller, W., Peindl, P., Moyschewitz, G., Wallbrecher, E., Thöni, M., 1992. Evolution of Lower Austroalpine units along eastern margins of the Alps. ALCAPA-Field Guide, Graz, pp. 97–114.

Neubauer, F., Dallmeyer, R.D., Dunkl, I., Schirnik, D., 1995. Late Cretaceous exhumation of the metamorphic Gleinalm dome, Eastern Alps: kinematics, cooling history and sedimentary response in a sinistral wrench corridor. Tectonophysics 242, 79–89.

Neubauer, F., Genser, J., Handler, R., 2000. The Eastern Alps: result of a two-stage collision process. Mitteilungen der Österreichischen Geologischen Gesellschaft 92, 117–134.

Passchier, C.W., Trouw, R.A.J., 1998. Microtectonics. Springer-Verlag, Berlin.

Price, G.P., 1985. Preferred orientations in quartzites. In: Wenk, H.-R. (Ed.). Preferred Orientations in Deformed Metals and Rocks: an Introtuction to Modern Texture Analysis. Academic Press, Orlando, pp. 385–406.

Ratschbacher, L., Frisch, W., Neubauer, F., Schmid, S.M., Neugebauer, J., 1989. Extension in compressional orogenic belts: the Eastern Alps. Geology 17, 404–407.

Ratschbacher, L., Hehrmann, J.H., Pahr, A., 1990. Penninic windows at the eastern end of the Alps and their relation to the intra-Carpathian basins. Tectonophysics 172, 91–105.

Riedmüller, G., 1967. Zur Geologie des NW-Teiles der Buckligen Welt, Ph.D. thesis, University of Vienna.

Ring, U., Ratschbacher, L., Frisch, W., 1988. Plate boundary kinematic in the Alps: motion in the Arosa suture zone. Geology 16, 696–698.

Rowe, K.J., Rutter, E.H., 1990. Paleostress estimation using calcite twinning: experimental calibration and application to nature. Journal of Structural Geology 12, 1–18.

Scharbert, S., 1990. Rb–Sr–Daten aus dem Raabalpenkristallin. Excursion Guide "Raabalpen- und Wechselkristallin der TSK III", 3. Symposium für Tektonik, Strukturgeologie, Kristallingeologie, Graz, pp. 22–26.

Schmid, S.M., Panozzo, R., Bauer, S., 1987. Simple shear experiments on calcite rocks: rheology and microfabric. Journal of Structural Geology 9, 747–778.

Tollmann, A., 1977. Geologie von Österreich, Die Zentralalpen. Deuticke, Vienna.

Tollmann, A., 1978. Eine Serie neuer tektonischer Fenster des Wechselsystems am Ostrand der Zentralalpen. Mitteilungen der Österreichischen Geologischen Gesellschaft 68, 129–142.

Wagreich, M., 1993. Subcrustal tectonic erosion in orogenic belts; a model for the Late Cretaceous subsidence of the northern Calcareous Alps (Austria). Geology 21, 941–944.

Wenk, H.R., Takeshita, T., Bechler, E., Erskine, B.G., Matthies, S., 1987. Pure shear and simple shear calcite textures. Comparison of experimental, theoretical and natural data. Journal of Structural Geology 9, 731–745.

Wieseneder, H., 1971. Gesteinsserien und Metamorphose im Ostabschnitt der österreichischen Zentralalpen. Verhandlungen der Geologischen Bundesanstalt 2, 344–357.

Williams, P.F., 1985. Multiply deformed terrains—problems of correlation. Journal of Structural Geology 7, 269–280.

Willingshofer, E., 1995. Strukturgeologische Entwicklung unterostalpiner tektonischer Fenster am Alpenostrand am Beispiel des Scheiblingkirchner Fensters (NÖ) [translated: Structural evolution of Lower Austroalpine tectonic windows at the eastern margin of the Alps on the example of the Schieblingkirchen Window (Lower Austria)]. Unpublished Master thesis, University of Graz.

Willingshofer, E., van Wees, J.D., Cloetingh, S.A.P.L., Neubauer, F., 1999a. Thermomechanical consequences of Cretaceous continent–continent collision in the eastern Alps (Austria): insights from two-dimensional modeling. Tectonics 18, 809–826.

Willingshofer, E., Neubauer, F., Cloetingh, S., 1999b. The significance of Gosau-type basins for the Late Cretaceous tectonic history of the Alpine–Carpathian Belt. Physics and Chemistry of the Earth 24, 687–695.